New Insights into the Self-Assembly of Insulin Amyloid Fibrils: An H−D Exchange FT-IR Study†

Wojciech Dzwolak,*,‡,§ Anna Loksztejn,‡,§ and Vytautas Smirnovas‡,||

Institute of High-Pressure Physics, Polish Academy of Sciences, Sokolowska 29/37, 01-142 Warsaw, Poland, and Department of Chemistry, Warsaw University, Pasteura 1, 02-093 Warsaw, Poland

Received February 18, 2006; Revised Manuscript Received April 18, 2006

ABSTRACT: The solvent protection of the amide backbone in bovine insulin fibrils was studied by FT-IR spectroscopy. In the mature fibrils, approximately 85 ± 2% of amide protons are protected. Of those "trapped" protons, a further 25 ± 2 or 35 ± 2% is H−D exchanged after incubation for 1 h at 1 GPa and 25 °C or 0.1 MPa and 100 °C, respectively. In contrast to the native or unfolded protein, fibrils do not H−D exchange upon incubation at 65 °C. A complete deuteration of H_2O-grown fibrils occurs when the β-sheet structure is reassembled in a 75 wt % DMSO/D_2O solution. Our findings suggest a densely packed environment around the amide protons involved in the intermolecular β-sheet motive. In disagreement with the concept of "amyloid fibers as water-filled nanotubes" [Perutz, M. F., et al. (2002) *Proc. Natl. Acad. Sci. U.S.A. 99*, 5591−5595], elution of D_2O-grown fibrils with H_2O is complete, which is reflected by the vanishing of D_2O bending vibrations at 1214 cm^{-1}. This implies the absence of "trapped water" within insulin fibrils. The rigid conformations of the native and fibrillar insulin contrast with transient intermediate states docking at the fibrils' ends. Room-temperature seeding is accompanied by an accelerated H−D exchange in insulin molecules in the act of docking and integrating with the seeds, proving that the profound structural disruption is the *sine qua non* of forming an aggregation-competent conformation.

Protein misfolding and amyloidogenesis are now known to play the central role in the etiology of several human disorders, such as Alzheimer's disease or Parkinson's disease. Amyloids, whether associated with disease or grown in vitro, are fibrillar, β-sheet-rich protein aggregates sharing many morphological and physicochemical traits. This holds true regardless of genetic origins, structure, and size of native precursors (*1*). While the understanding of mechanisms of amyloidogenesis and relations between misfolding and the disease has advanced recently, many questions remain unanswered. A considerable body of evidence suggests that conversion of any protein, even with a marginal propensity to fold into β-sheets (*2*, *3*), into fibrils is only a question of finding appropriate experimental conditions. The structural patterns of amyloids invariably employ backbone chain interactions, implying that protein fibrillation may be a common, generic feature of proteins as polyamides (*4*).

Some aspects of amyloidogenesis, such as the conformational basis of the HET-s[1] prion infectivity (*5*, *6*) or the dynamic character of fibrillation (*7*), have been approached by means of NMR spectroscopy or mass spectrometry coupled to a H−D exchange technique, which itself is long established in the field of protein folding (*8*, *9*). A particular advantage of the H−D exchange lies in its capacity to characterize transient conformations, which may represent a negligible (and therefore difficult to detect) fraction of all protein molecules. The H−D exchange technique has been employed in mapping core structures of β2-microglobulin (*10*, *11*) and Alzheimer amyloid fibrils (*12*) by NMR spectroscopy. The method proved to be equally revealing in MS studies of order−disorder boundaries in fibrils formed by α-synuclein (*13*) and Alzheimer peptide mutants (*14*). However, applications of either method are limited to homogeneous samples containing rather low molecular mass species. Unless preliminary separation is involved, it is necessary to dissociate solvent-exchanged fibrils [e.g., by dissolving them in concentrated DMSO (*7*, *10*, *11*)] or focus on the earliest stages of amyloidogenesis, when small oligomers prevail (*15*). In contrast to NMR spectroscopy and MS spectrometry, FT-IR spectroscopy is a global conformational probe allowing one to trace protein aggregation continuously from its earliest stages until formation of mature amyloid fibrils. Because FT-IR, unlike CD, is sensitive to the polarity of strand-to-strand arrangements in β-sheets and to the strength of inter-β-strand hydrogen bonding, the method is suitable for monitoring fibrillation of natively β-sheet-rich proteins (*16*) and distinguishing between different amyloid "strains" (*17*). The FT-IR method is not site-specific with respect to H−D exchange, as a time-dependent decay of amide II band accounts for all amide protons

† Financial support from the Polish Ministry of Education and Science [Grant 2P04A 011 28 (2005−2007)] is gratefully acknowledged.

* To whom correspondence should be addressed. Phone: +48 22 888 0237. Fax: +48 22 632 4218. E-mail: wdzwolak@unipress.waw.pl.

‡ Polish Academy of Sciences.

§ Warsaw University.

|| Present address: Department of Chemistry, Physical Chemistry I-Biophysical Chemistry, University of Dortmund, Otto-Hahn Str. 6, D-44227 Dortmund, Germany.

[1] Abbreviations: CD, circular dichroism; DMSO, dimethyl sulfoxide; FT-IR, Fourier transform infrared; HET-s, prion from *Podospora anserina*; HHBW, half-height bandwidth; MS, mass spectrometry; NMR, nuclear magnetic resonance; TEM, transmission electron microscopy.

10.1021/bi060341a CCC: $33.50
Published on Web 06/06/2006

replaced with deuterons. In protein folding studies, FT-IR-monitored H−D exchange is a routine probe of the stability of tertiary contacts. Recently, this approach has been used to study the compactness of aggregation-prone intermediates (*18*) and solvent protection in mature β2-microglobulin fibrils (*19*).

The physiological importance, the wealth of structural and biochemical data, and the predisposition to fibrillate in vitro have contributed to insulin becoming one of the workhorse protein models in the field of amyloid research. At the same time, in vivo fibrillation of insulin is rare and per se does not seem to pose serious medical problems (*20*). Under physiological conditions, insulin is stored as Zn^{2+}-coordinating hexamers. At low pH, tetramers and dimers are promoted (*21*); 20% acetic acid or ethanol at pH 2 dissociates insulin to monomers (*21*−*23*), each consisting of two: 21- and 30-residue polypeptide chains connected by two disulfide bridges. Insulin aggregation is enhanced by conditions favoring partly destabilized monomers and dimers, such as high temperature and low pH (*24*), the presence of denaturants (*25*, *26*), or hydrophobic media (*27*). Such conditions promote bulky, partly unfolded, and fibrillation-prone monomers (*25*). The formation and clumping of aggregation-prone monomers are spatially demanding, which explains why high hydrostatic pressure disfavors this process (*18*). DSC studies have shown that insulin aggregation in aqueous samples is exothermic, although it is preceded by endothermic unfolding (*18*). Overall, the fibrillation is energetically self-sustaining and therefore may be accomplished by seeding of monomers or dimers at room temperature with preformed amyloid templates (*17*). While the presence of fine infrared features depends on particular conditions of the growth of fibrils, the typical infrared spectra suggest a parallel arrangement of β-strands, which is in accordance with structural models proposed for insulin fibrils (*28*).

Dynamics of aggregation-prone conformations and the structural basis of fibril stability are the two obscure aspects of insulin amyloidogenesis addressed in this study by the means of FT-IR spectroscopy combined with H−D exchange. Here we show that this approach, when applied to a seeded fibrillation under ambient conditions, provides a new insight into the critical amount of structural disruption necessary for an aggregation intermediate to be formed. When effects of pressure, temperature, and DMSO on insulin fibrils were examined, FT-IR coupled to H−D exchange has been employed as a more adequate probe of conformational stability than the infrared spectroscopy alone. On the other hand, we have taken advantage of infrared bending bands assigned to D_2O molecules to examine the presence of trapped water in cavities of the stacked insulin conformations. This knowledge is urgently needed to deepen our understanding of the role of void volumes in the stability, biological activity, and possible biotechnological applications of amyloids.

MATERIALS AND METHODS

Insulin Fibrils for Seeding (Amyloid[D]). Bovine pancreatic insulin from Sigma was incubated at 5 wt % in 0.1 M NaCl in D_2O (pD 1.8) [or in 0.1 M NaCl in 20 wt % EtOD/D_2O (pD 1.8)] at 60 °C for 48 h. The presence of mature amyloid was confirmed by TEM, CD, and ThT fluorescence measurements. Fibrils formed under this set of conditions contained completely deuterated amide bonds, as reflected by the lack of infrared absorption around 1550 cm^{-1}. For kinetic H−D exchange experiments, the fully deuterated fibrils were sonicated for 5 min before being rapidly mixed with a native insulin solution.

Insulin Fibrils for Pressure-, Temperature-, and DMSO-Assisted H−D Exchange (Amyloid[H]). Amyloid samples were prepared according to the same procedure, except that the protein concentration was 2 wt % and no deuterated compounds were used. Amyloid[H] samples were briefly sonicated, then centrifuged, and resuspended in 0.1 M NaCl in D_2O (pD 1.8). This routine was repeated several times until bulk H_2O was completely eluted (as judged by the intensity of the −OH stretching band around 3400 cm^{-1}). The final precipitate was estimated to be 10 wt % Amyloid-[H] in 0.1 M NaCl in D_2O (pD 1.8).

Temperature, Pressure, and DMSO-Assisted H−D Exchange in Amyloid[H]. Fresh preparations of Amyloid[H] in 0.1 M NaCl in D_2O were incubated at ambient pressure and 100 °C, or at 1 GPa at 25 °C, using a homemade high-pressure system. Immediately after each incubation, acquisition of FT-IR spectra followed. For experiments with DMSO, a sample of 10 wt % Amyloid[H] gel in 0.1 M NaCl in D_2O (pD 1.8) was mixed with pure, water-free DMSO (from Aldrich) to produce a final DMSO concentration of 75 wt %. Upon being mixed with the cosolvent, the opaque amyloid precipitate dissolved quickly, producing a transparent sample. The amyloid dissolved in the mixture of D_2O and DMSO was immediately injected into to a thermostated flow-through FT-IR cell. Temperature scans were performed in the range of 15−65 °C at a rate of 20 °C/h.

Kinetics of the Seed-Induced Fibrillation and H−D Exchange. For seeding experiments, a 5 wt % solution of native insulin in 0.1 M NaCl and D_2O (pD 1.8) or in 0.1 M NaCl and a 20 wt % EtOD/D_2O solution (pD 1.8) were prepared immediately before measurements. The "seeded" samples contained an addition of 20 wt % freshly sonicated amyloid formed spontaneously at 60 °C under the same solvent conditions as described in Insulin Fibrils for Seeding (Amyloid [D]). Native insulin samples were rapidly mixed with amyloid and were injected through a flow-through system into a thermostated FT-IR CaF_2 cell. The lag time between the preparation of fresh insulin samples (with or without Amyloid[D] seeds) and the initiation of kinetic measurements was 5 min. Throughout the first 20 h of the kinetic experiments, the temperature in the FT-IR cell was stabilized at 25 °C. Subsequently, the cell was heated to 60 °C at a constant rate of 40 °C/h, kept for 1 h at 60 °C, and finally cooled to 25 °C. FT-IR spectra were collected every 5 min during the combined 23 h of a single kinetic scan.

FT-IR Spectroscopy. For most FT-IR measurements, a CaF_2 transmission cell was equipped with 0.05 mm Teflon spacers. Thinner 0.006 mm spacers were used for acquisition of the infrared spectra of H_2O, D_2O, their equimolar mixture (Supporting Information), and *A*myloid[H] fibrils dissolved in H_2O. A 0.1 mm spacer was used to investigate the D−O−D bending band in centrifuged Amyloid[D] fibrils resuspended in H_2O at a concentration of ∼10 wt %. The temperature in the cell was controlled through an external water circuit connected to a PC-controlled thermostat. All the FT-IR spectra were collected on a Nicolet NEXUS

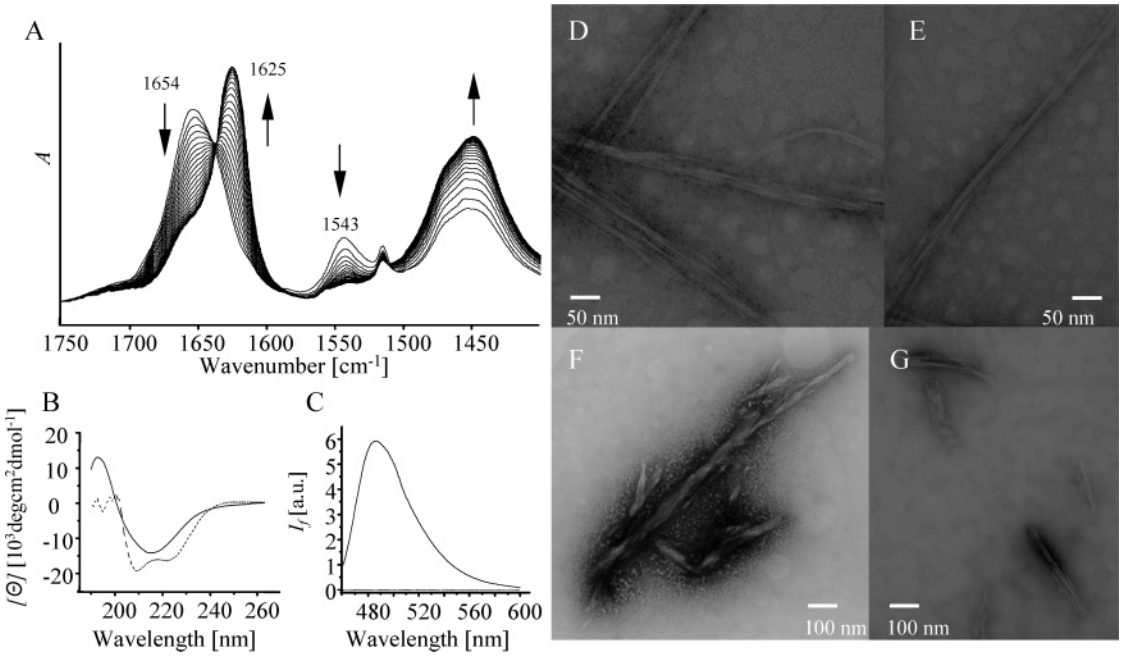

FIGURE 1: (A) Time-resolved FT-IR spectra show amide I and amide II vibrational bands of bovine insulin undergoing seed-induced aggregation at 25 °C in 0.1 M NaCl and D_2O (pD 1.8). The arrows indicate directions of spectral change. (B and C) Insulin at 25 °C, 0.1 M NaCl, and pD 1.8 before (- - -) and after complete fibrillation (—) probed by CD (B) and fluorescence emission of ThT (C). (D−F) Negatively stained TEM images of mature insulin amyloid fibrils formed in the aqueous (D and E) and ethanol-containing preparations (F). (G) Amyloid seeds produced through sonication of mature amyloid.

FT-IR spectrometer equipped with a liquid nitrogen-cooled MCT detector. Typically, for a single spectrum, 256 interferograms of 2 cm^{-1} resolution were co-added. For sufficient-quality D−O−D bending spectra of Amyloid[D] in H_2O, 1024 interferograms were required. During the measurement, the sample chamber was continuously purged with CO_2-free dry air. From each sample's spectrum, corresponding buffer and water vapor spectra were subtracted. Spectra were baseline-corrected and normalized according to the integral intensity of the amide I band. Semiquantitative plots of the progress of α-helix to β-sheet refolding upon aggregation were calculated as $(I - I_\alpha)/(I_\beta - I_\alpha)$, where I_α is the spectral intensity at a wavenumber assigned to the β-sheet (ca. 1625 cm^{-1}) in native insulin (the first spectrum), I_β is the intensity after complete aggregation, and I is a transient intensity. Data processing was performed with GRAMS (ThermoNicolet). All details regarding the methodology of infrared detection of water trapped within amyloid fibrils are described in the Supporting Information and the legend of Figure 5.

CD Spectroscopy and Thioflavin T Fluorescence. For CD measurements, 1 mm path length quartz cuvettes were used. Protein samples were diluted with 0.1 M NaCl in D_2O (pD 1.8) to a final concentration of 0.05 wt %. Spectra were acquired at 25 °C on a Jasco 715 CD spectrometer. Measurements of fluorescence emission spectra of ThT bound to amyloid fibrils were carried out according to the routine protocols (*18*). Diluted samples contained 0.03 wt % protein and 10^{-4} wt % ThT in 0.1 M NaCl and D_2O (pD 1.8). Emission spectra were collected at 25 °C on an AMINCO Bowman Series 2 luminescence spectrometer (excitation at 450 nm, three repetitions) equipped with 10 mm path length quartz cuvettes.

Transmission Electron Microscopy (TEM). The samples of insulin amyloid formed under the conditions described above in the FT-IR section were diluted 10-fold prior to being applied onto Formvar carbon-coated 400 mesh/in. copper grids. The samples were left to adsorb for 30 s. Excess material was removed through a triplicate wash-off with the buffer. In the following step, the remaining specimens were negatively stained with a 1 wt % uranyl acetate solution. After 60 s, the excess stain was removed and the grid was left to dry. The fibrils were examined on a Joel JEM 1200 EX transmission electron microscope at an accelerating voltage of 80 kV and at a nominal magnifications of 40000× and 100000×.

RESULTS

Figure 1A shows time-dependent changes in amide I and II vibrational bands of native, undeuterated insulin in D_2O seeded with preformed amyloid at 25 °C. The characteristic shifting of the amide I band from 1654 to 1625 cm^{-1} reflects refolding of the native, predominantly helical structure into stacked β-strands. The conversion of the native protein into amyloid is completed within 3−4 h. The presence of fibrils is confirmed by CD (Figure 1B), the strong fluorescence of amyloid-bound thioflavin T (Figure 1C), and TEM images of negatively stained protein samples (Figure 1D−G). The conformational transition is accompanied by a simultaneous decay of the amide II band at 1550 cm^{-1} and the appearance of the band at 1450 cm^{-1}, which is indicative of an ongoing H−D exchange of amide protons. Because even unseeded native insulin in D_2O undergoes H−D exchange, it is crucial to compare relative rates of the backbone's deuteration in fibrillating (seeded) and intact (unseeded) protein samples. The effects of seeding on kinetics of the H−D exchange are presented in Figure 2A, where the remaining intensity of the 1550 cm^{-1} band approximates the number of nonexchanged amide protons. The experiments were carried out

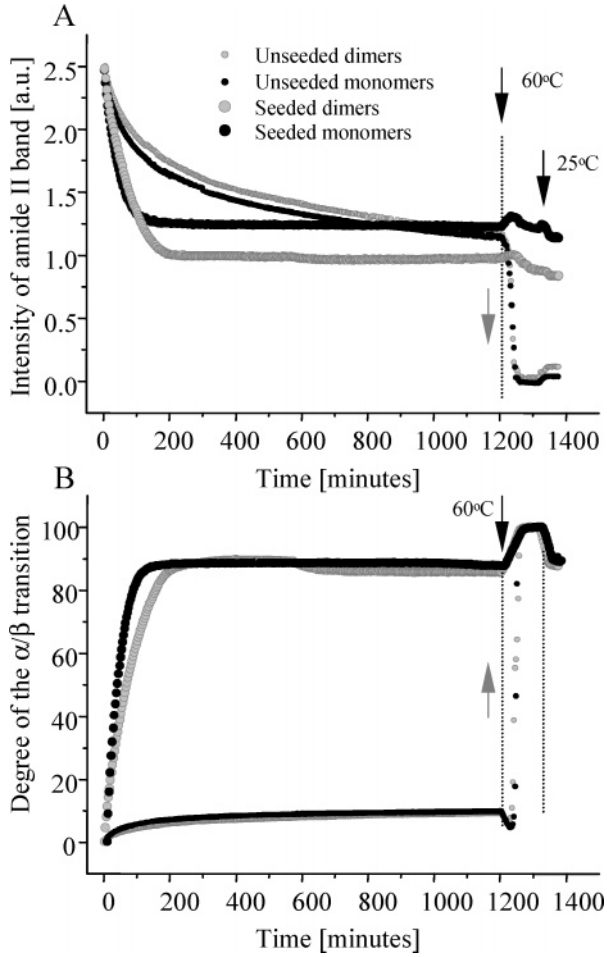

FIGURE 2: Effects of seeding on kinetics of deuteration (A) and aggregation (B) of insulin dimers [in 0.1 M NaCl and D_2O (pD 1.8)] and monomers [0.1 M NaCl in 20 wt % EtOD with D_2O (pD 1.8)]. At 25 °C, maintained during the first 1200 min of incubation, only the seeded samples aggregated (B), which was accompanied by acceleration in the rate of H−D exchange (A). The residual intensity of the amide II band corresponds to some amyloid-trapped amide protons, which do not solvent exchange upon heating at 60 °C. The unseeded samples undergo fast temperature-induced aggregation and a simultaneous deuteration.

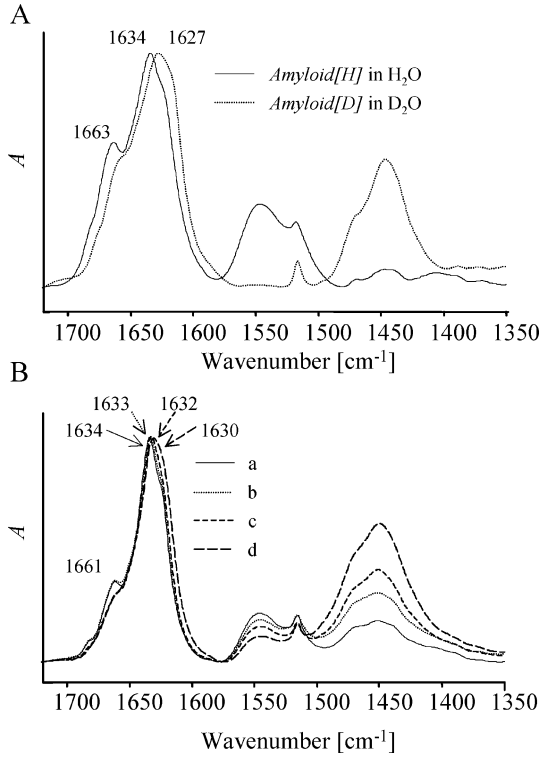

FIGURE 3: (A) FT-IR spectra of Amyloid[H] and Amyloid[D] grown at 60 °C in H_2O and D_2O, respectively. The complete deuteration of the peptide backbone results in a minor red shift of the amide I band and a major shift of the amide II band. The ratios of relative intensities of the amide I and II bands are 3.35:1 for undeuterated and 2.54:1 for the deuterated amyloid. (B) FT-IR spectra of Amyloid[H] resuspended in 0.1 M NaCl and D_2O (pD 1.8) and subjected to H−D exchange enhancing influences of temperature and pressure: (a) control spectra, (b) spectra after 1 h at 1 GPa and 25 °C, (c) spectra after 1 h at 100 °C, and (d) spectra after incubation for 3 h at 100 °C. According to these spectra, intensities of the amide II band in panel B are 25% (a), 19% (b), 16% (c), and 9% (d) of that of the amide I band (±1%).

in the absence and presence of 20 wt % ethanol, which is known to dissociate insulin dimers (*22*, *23*, *29*). For each experimental set of data, progress of the simultaneous conformational transition is plotted according to the intensity of the spectral component assigned to the *β*-pleated conformation (Figure 2B). The temperature was kept at 25 °C for the first 20 h of the FT-IR-monitored process, then increased to 60 °C at a rate of 40 °C/h, and finally decreased to room temperature. Plateaus of the solvent exchange plots in Figure 2A clearly coincide with the completion of fibrillation (Figure 2B), which occurs after 2 and 3 h for monomers (samples in 20 wt % ethanol) and dimers (aqueous samples), respectively. Under the ambient conditions (25 °C) and in the absence of amyloid templates, insulin retains its native conformation and a number of slowly exchanging amide protons. The transient increase in temperature to 60 °C causes immediate aggregation and almost complete H−D exchange in unseeded protein samples. The temperature jump has very little effect on the seeded and, by that time, completely fibrillated samples (Figure 2A). To assess the stability and solvent protection of the amyloid with respect to physicochemical factors known to disrupt protein fibrils, such as high temperature (*30*, *31*), high pressure (*32*), and DMSO (*33*), further experiments were conducted.

FT-IR spectra of insulin amyloid grown in light and heavy water are shown in Figure 3A. Substitution of all amide protons with deuterons results in the complete vanishing of the amide II band at 1550 cm^{-1}. The small persistent peak at 1516 cm^{-1} corresponds to the four tyrosine residues present in insulin monomer (*34*). To some extent, the deuteration also affects the amide I band, which shifts from 1634 to 1627 cm^{-1} while a minor peak around 1663 cm^{-1} assigned to loops disappears. Corrected for the overlapping tyrosine peak, the integral intensity of the amide II band of Amyloid[H] is approximately 30% of the amide I band intensity. The ratio is expected to vary for fibrils obtained from different proteins, as the "integral intensity" of the amide I band is not corrected for overlapping contributions of side chains, which, while minor, vary between proteins. According to spectra in Figure 3B, the intensity of the 1550 cm^{-1} peaks shrinks to 25% of the amide I band's intensity immediately after resuspension of Amyloid[H] in heavy water, which corresponds to exchange of roughly 17% of amide protons. Under the ambient conditions, once the fibrils are dispersed in D_2O, after the initial decay of the amide II intensity, no further spectral symptoms of ongoing deutera-

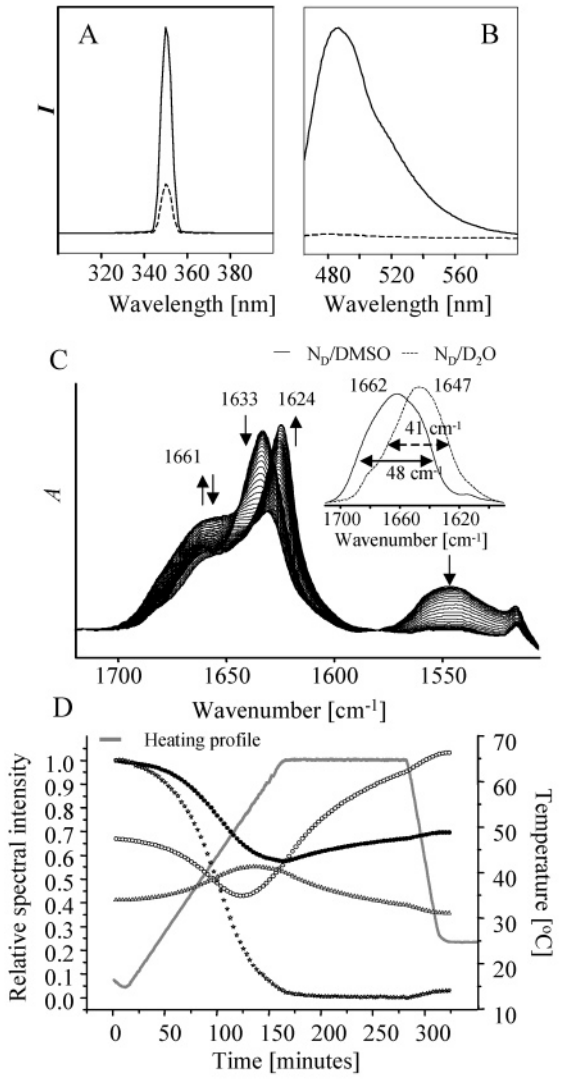

FIGURE 4: Scattering, $\lambda_{350\ nm}$, fluorescence emission of ThT (A) and of Amyloid[H] (B) in water (—) and 75 wt % DMSO (- - -). (C) FT-IR spectra of 2.5 wt % Amyloid[H] in a mixture of 0.1 M NaCl in D_2O (pD 1.8) and DMSO (1:3) upon gradual heating from 15 to 65 °C at a rate of 20 °C/h. The inset shows superimposed FT-IR spectra of 2 wt % solvent-exchanged native insulin dissolved in pure DMSO or in D_2O (pD 1.8). (D) Relative spectral intensity changes at the wavenumbers assigned to three conformational components of insulin amyloid heated in the D_2O/DMSO solution: (black circles) pre-transition β-sheet, 1633 cm^{-1}; (gray triangles) DMSO-solvated random coil, 1660 cm^{-1}; (white circles) final β-sheet, 1624 cm^{-1}; (white stars) simultaneously decaying amide II band at 1550 cm^{-1}.

tion are observed. This suggests that from a kinetic standpoint, the amide protons of insulin amyloid can be roughly categorized as either solvent-exposed or strongly solvent-protected. As Figure 3B shows, H−D exchange is promoted to some extent by high hydrostatic pressure or high temperature. A small peak around 1663 cm^{-1} assigned to loops and turns in the undeuterated amyloid shifts immediately to 1661 cm^{-1} upon resuspension in D_2O and vanishes altogether after the brief heating.

DMSO has a more radical effect on insulin fibrils than either high pressure or high temperature. When DMSO is mixed with a suspension of Amyloid[H] in D_2O, the opaque protein sample becomes translucent within seconds. Figure 4A reveals a more than quadruple decrease in scattering at 350 nm of the Amyloid[H] dissolved in 75 wt % DMSO compared with that of an aqueous sample. This is followed by a roughly 60-fold decrease in the fluorescence intensity of fibril-bound ThT (Figure 4B). However, the presence of the amide I peak at 1633 cm^{-1} in the first FT-IR spectrum recorded for the freshly dissolved amyloid at 15 °C in the DMSO/water mixture (Figure 4C) is a sign that β-sheet remains the major secondary structure component of the protein. The DMSO/D_2O solution of insulin fibrils was subjected to gradual heating to 65 °C at a rate of 20 °C/h followed by an isothermal 2 h incubation, and consecutive cooling to 25 °C. Conformational transitions were monitored by infrared spectra stacked in Figure 4C. The major spectral changes evoked by the changing temperature include dramatic shifting of the amide I band maximum from 1633 to 1624 cm^{-1}, vanishing of the amide II band at 1550 cm^{-1}, and a transient increase in absorption at 1661 cm^{-1}. In the inset of Figure 4C, spectra of native fully deuterated insulin dissolved in pure DMSO and in D_2O are compared. The replacement of heavy water with DMSO results in a marked broadening of the peak by roughly 17% (HHBW) and a blue shift of the peak's maximum to 1662 cm^{-1}, which corresponds to free carbonyl groups of peptide bonds in DMSO-solvated random coil conformations (*35*). Figure 4D depicts time-dependent changes in the spectral components at 1633, 1660, 1624, and 1550 cm^{-1}, thereby providing quantification of the major conformational transitions, as well as the accompanying H−D exchange. Increasing temperature promotes the DMSO-solvated random coil at the expense of the β-sheet structure at 1633 cm^{-1}. The gradual decay of the latter band is clearly in phase with the complete vanishing of the amide II peak. According to Figure 4D, deuteration is complete before the heating profile reaches the plateau. During the following isothermal incubation at 65 °C, the time-dependent conformational transition occurs, which is reflected by the steep increase in intensity at 1624 cm^{-1}.

Figure 5A shows original (without solvent subtraction) FT-IR spectra of insulin fibrils grown in D_2O gradually eluted with H_2O. Should a sample of D_2O-grown fibrils be eluted with another solvent, the persisting spectral intensity around 1205−1215 cm^{-1} would correspond to an amount of trapped water. Using H_2O as an eluant is particularly advantageous because of the dynamic equilibrium among the three molecules: H_2O, D_2O, and HDO (see the Supporting Information). The resulting quadratic dependencies of their molar fractions (*36*, *37*) enable effective spectral "quenching" of unprotected heavy water, while the bending vibrations of water (D_2O) molecules sequestered from the bulk eluant (H_2O) by fibrous topology will give rise to the peak at 1214 cm^{-1} (the approach is explained in the Supporting Information). In the first bottom spectrum recorded before the first round of elution, the amide I band at 1627 cm^{-1}, the tiny tyrosine peak at 1516 cm^{-1}, the fully deuterated amide II band at 1450 cm^{-1}, and the large peak corresponding to the bending vibrations of the bulk solvent (D_2O) above 1200 cm^{-1} are seen. As the following spectra prove, adding H_2O results in dramatic spectral changes: the magnitude of the D_2O band rapidly decreases, while the peaks around 1650 and 1450 cm^{-1} gain intensity. These are consequences of the amide I and amide II bands being overlapped by the bending vibrations of H_2O and HDO, respectively. In H_2O/D_2O mixtures, the HDO band is most intense at the equimolar

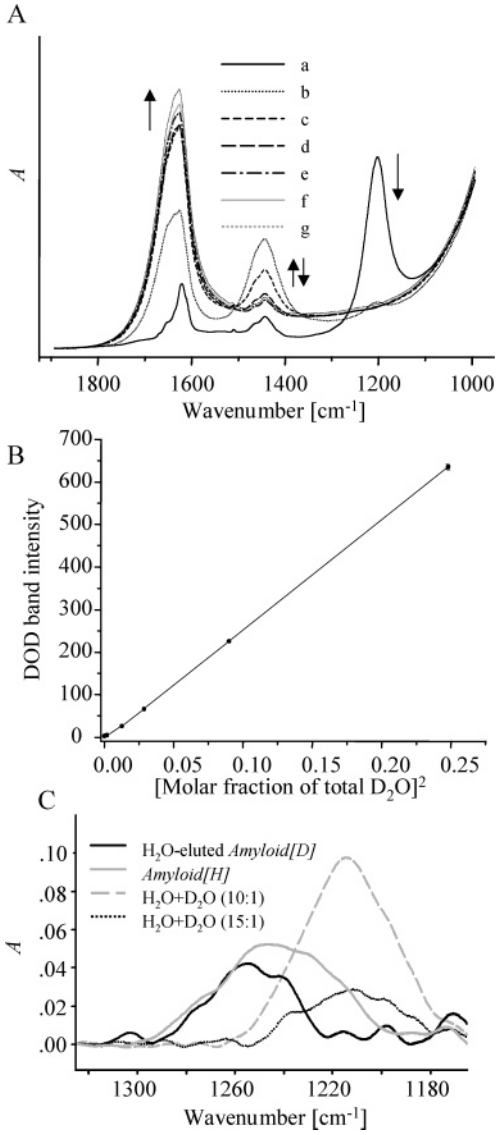

FIGURE 5: (A) Original (without solvent subtraction) FT-IR spectra of Amyloid[D] separated from the excess of D_2O and resuspended several times in H_2O (pH 1.8) and 0.1 M NaCl. Spectra collected on a short optical length using 0.006 mm spacers. The total concentration of D_2O expressed as a molar fraction is (a) 1, (b) 0.5, (c) 0.29, (d) 0.16, (e) 0.11, (f) 0.07, and (g) 0.03. (B) Integral intensity of the DOD bending band at 1214 cm^{-1} plotted vs the square of the remaining D_2O molar fraction after consecutive elution steps. (C) The spectrum of Amyloid[H] overlapped with the spectrum of Amyloid[D] after complete elution with H_2O. Superimposed are spectra of D_2O dispersed in H_2O at effective molar fractions of 0.01 and 0.0044, obtained through mixing of H_2O and D_2O at 10:1 and 15:1 molar ratios, respectively.

ratio of protons and deuterons but decreases when the molar ratio of H (H_2O) increases further (Supporting Information). In Figure 5A, this is reflected by a gradual decrease of the magnitude of the 1450 cm^{-1} band back to the initial intensity of the amide II band. The superimposition of the H_2O bending band and protein amide I band explains why the experimental approach implemented in this study (D_2O-grown fibrils eluted with H_2O) cannot be replaced with the alternative, H_2O-grown fibrils eluted with D_2O. In Figure 5B, a quantitative dependence of the integral intensity of the D_2O band centered around 1214 cm^{-1} is plotted as a function of the square of the total molar ratio of D_2O according to the spectra from Figure 5A. As expected, the plot is linear. It can be easily rationalized that this linearity holds true as long as all D_2O molecules participate in the equilibrium with H_2O and HDO. Should there be a fraction of D_2O trapped and therefore prevented from the exchange with H_2O, an extrapolation of the plot to an infinitive elution with H_2O [and therefore (molar fraction of total $D_2O)^2 = 0$] would cross the ordinate axis above (0,0), at the D_2O band intensity corresponding to an amount of water trapped by the fibrils. In Figure 5C, completely H_2O-eluted spectra of D_2O-grown amyloid and fresh H_2O-grown amyloid are juxtaposed along with infrared spectra of H_2O/D_2O mixtures at 10:1 and 15:1 molar ratios corresponding to effective molar fractions of spectrally detectable D_2O of 0.01 and 0.0044, respectively. It is clear that the H_2O-washed D_2O-grown amyloid does not exhibit the spectral characteristics around 1214 cm^{-1} expected for trapped D_2O. The minor absorption around 1250−1260 cm^{-1} is a feature present in both the deuterated and nondeuterated amyloid samples and, thus, not related to the possible presence of heavy water. The band can be assigned to another group of stretching vibrations in tyrosine side chains (*34*).

DISCUSSION

Solvent Exchange in the Intermediate State. According to the data presented in Figures 2 and 3, most of the amide protons in insulin amyloid are firmly protected within the fibrous and apparently temperature resistant structure. The data shown in Figure 2 imply a small degree of solvent protection and, thereby, a high degree of structural disorder in the intermediate state formed transiently by free insulin molecules docking and integrating with the fibrils during the elongation. This effect is clearly not related to a possible dissociation of dimers prior to fibrillation, as the data obtained for ethanol-dissolved and thus monomeric protein permit us to draw the same conclusion. Although the β-sheet conformation prevails in fibrils, it is not the sole contributor to an overall intensity of the amide I band. Because molar absorption coefficients for various secondary structures may differ by up to 20% (*38*), deviations from the 30% ratio of intensities of the amide II and amide I bands (Figure 3A) are expected. Nevertheless, for a given protein, the intensity of the amide II band at 1550 cm^{-1} related to the amide I band as an internal spectral standard is a useful gauge of total solvent protection, permitting comparisons between protein conformers (*19*).

Solvent Protection of Insulin Fibrils. The spontaneous partial deuteration of Amyloid[H] upon resuspension in heavy water is fast, and solvent exchange does not seem to proceed further at room temperature, suggesting that the remaining 83% of amide protons are strongly protected (Figure 3). Interestingly, a brief sonication of amyloid, which breaks fibrils, does not seem to change this ratio either, implying that, unlike in the case of fibrils formed by the SH3 domain protein (*7*), but in accordance with an earlier Raman study on insulin fibrils (*39*), dynamic dissociation and reassociation of ingredient insulin monomers are relatively damped.

Loops are more likely to be solvent-exposed and more susceptible to thermal fluctuations. Thus, rather unsurprisingly, such less-ordered structures undergo H−D exchange first (Figure 3B). The prolonged high-temperature incubation

further promotes H−D exchange in the fibrils. This, however, despite extreme pD conditions, does not lead to any visible deterioration of the protein in terms of conformation (intact amide I band) or covalent bonds. The latter may be inferred from the lack of any absorbance above 1710 cm^{-1}, where stretching bands of −COOD formed from hydrolyzed (in D_2O, and at this low pD) amide groups would inevitably appear (*34*).

Since both high-pressure and high-temperature treatment proved to be incapable of inducing complete deuteration of insulin fibrils, an alternative means of enhancement of H−D exchange was sought. Some chemical denaturants, such as urea or guanidinium hydrochloride, are ruled out because of the strong spectral overlap with amide I and amide II vibrational bands. Since DMSO does not absorb in this critical spectral region, it was applied in this work. DMSO has been used at a concentration in heavy water approaching the level used for the rapid dissolving of β2-microglobulin fibrils (*10*, *11*). The specific mechanisms of the effect of DMSO on protein (strong competitive hydrogen bonding) make it rather ineffective in dissociating fibrils at its low concentration (free water molecules). On the other hand, an extremely high (>85 wt %) concentration causes an overly rapid dissociation and H−D exchange hampering time-resolved monitoring of the process. In addition, an appreciable amount of D_2O provides deuterons necessary for an efficient tracing of H−D exchange process. A 75 wt % DMSO/D_2O mixture is an optimum condition for carrying out a complete, DMSO-assisted temperature-induced deuteration of insulin fibrils. Unlike helix-promoting fluorinated alcohols known to dissociate amyloid fibrils (*40*) according to poorly understood mechanisms, DMSO, a potent acceptor of hydrogen bonds, acts in a more straightforward manner. In aqueous protein samples and at a very high concentration (needed for saturation of water's hydrogen bonds), DMSO competes for amide's hydrogens with carbonyl groups. This leads to a complete breakage of protein secondary structure, which is supported by intramolecular (in native proteins) or intermolecular (in amyloids) hydrogen bonding. The simultaneous release of free carbonyl groups gives rise to the characteristic strong infrared band at 1662 cm^{-1} (*35*). The juxtaposition of panels A−C of Figure 4 is very revealing in terms of the character of the conformational transition induced in insulin fibrils by 75 wt % DMSO. The 4-fold decreased UV scattering intensity and the almost 60-fold decrease in amyloid-bound ThT fluorescence imply disintegration of the fibrils into less-ordered protein agglomerates (DMSO does not quench ThT fluorescence). The FT-IR spectra of the freshly DMSO dissolved fibrils show that β-sheet remains the dominant conformational motive. The marked absorption centered around 1550 cm^{-1} reflects the presence of unexchanged amide hydrogens, remaining abundant despite the vanishing of the fibrillar trap. The appearance of insulin's free carbonyl groups in the DMSO-solvated random coil state (*35*) is manifested by the broadening of the amide I peak by 17% (HHBW) and its blue shift to 1662 cm^{-1}. However, the presence of turns, which coincidentally absorb at the same wavenumber, cannot be ruled out. The cooperativity of H−D exchange and unfolding of β-sheet (Figure 4C) can be easily reconciled with the protected amide protons being directly involved in formation of the β-pleated structure. Likewise, a high degree of solvent protection of core β-sheet motives in Aβ (*12*, *14*) and α-synuclein (*13*) fibrils has been described previously. Interestingly, the peak at 1624 cm^{-1} assigned to deuterated β-sheet is continuing to gain intensity, while the intensity of the disordered conformation band (at 1660 cm^{-1}) is decreasing simultaneously (Figure 4C). Given that these events are taking place in the fully deuterated protein, while the peak of the newly formed β-sheet structure is visibly red-shifted compared to the aqueous preparations of the fully deuterated insulin amyloid (vide 1627 cm^{-1} according to Figure 3A), the H−D exchange does not seem to be the only cause of the spectral differences between the initial and final β-sheet (Figure 4C). Since a red shift of the amide I band is interpreted in terms of strengthening interstrand hydrogen bonding, it seems likely that prolonged heating of the disordered insulin in a concentrated DMSO/D_2O solution promotes a rearranged and environment-adopted extended structure, which is capable of withstanding the dissociating effect of DMSO. The final protein conformer did not, however, reveal any evidence of fibrils (data not shown). We have shown recently that a high concentration of ethanol promotes, presumably through extensive solvation of the side chains, β-pleated yet amorphous insulin aggregates (*29*). In DMSO, a solvent expected to bind directly to amide hydrogens and, through this, disrupt main chain interactions supporting the fibrils, a rearrangement of the extended structure leading to species with solvent-sequestered amide bonds (as evidenced by the presence of β-sheet in the spectra, Figure 4C) is puzzling. It may be hypothesized that under the particular conditions (e.g., equimolar with DMSO in the presence of water), a thermodynamic stability of such low-molecular mass soluble β-sheet-rich oligomers is achieved by, in part, hydrogen bonding between DMSO and insulin side chains.

Probing the Cavities of Insulin Fibrils. Apart from amide groups and polar side chains, water molecules trapped within fibrils' cavities constitute yet another form of molecular storage of exchangeable hydrogen atoms. An explicit idea that "amyloid fibers are water-filled nanotubes" has been put forward by Perutz and co-workers (*41*). In fact, other studies have revealed either a spacious central canal alongside mature amyloid fibrils (*42*) or abundant water molecules trapped between "wet" β-sheets formed by crystallization of amyloidogenic peptide (*43*). However, in the latter case, the water molecules were trapped within the crystal lattice on wet interfaces, which are not expected in a structure of regular amyloid fibers (*43*). The problem of whether fibrils' cavities are filled with water is of paramount importance for a number of reasons. First, as the increasing solvent entropy is said to be one of the driving forces of amyloidogenesis, the presence of highly restricted water molecules retained within amyloid cavities could offset gains in solvent entropy and tune thermodynamics of fibrillation. Second, the stability of amyloid against pressure, among other factors, is expected to depend on the presence of water in amyloid cavities. Third, this problem needs to be addressed when possible applications of fibrils in nanotechnology and as drug delivery media are considered. The capacity of FT-IR to detect whole water molecules (possibly trapped within amyloid fibrils) is useful in addressing these problems. The data presented in panels B and C of Figure 5 do not support the "trapped water" concept. Because the limit of detection primarily depends on the intensity of the D_2O peak relative to the "background"

absorption, it was necessary to compare the spectra of amyloid after the final elution step with a H_2O/D_2O mixture containing D_2O molecules at a concentration anticipated for the "nanotubes" filled with water. A calculation of a mass ratio relating the amount of amyloid to the amount of trapped water requires certain assumptions, as detailed structural data on insulin fibrils are lacking. This task was relatively easier in the case of sequence-less poly(L-glutamine) fibrils when all side chains are identical and contribute the same volumes inside and outside the β-helix-like well (*41*). While the van der Waals volume of the glutamine residue (*4*) is slightly larger than an average side chain volume in insulin, morphological (*44*) and possible structural (also in terms of three-dimensional packing) similarities (*28*) encourage the use of the poly(L-glutamine) fibrils as an approximate model for an estimation of water content in insulin fibrils. Because electron microscopy (*28*) gives a more reliable estimation of amyloid size than atomic force microscopy (*44*), we took 3 and 1.2 nm to be the outside and inside diameters of the fibrils, respectively. Given the partial specific volume of insulin, 0.71 cm^3/g (*18*), the maximal water content in insulin amyloid fibrils is 10 wt % of the whole protein mass. A protein sample, such as those used for infrared measurements in Figure 5A−C, containing roughly 10 wt % amyloid (Materials and Methods) may trap up to 1 wt % D_2O. This would correspond to a H_2O/D_2O mixture containing effectively 1% of D_2O molecules, i.e., mixed at a 10:1 molar ratio (Supporting Information). Estimation of an expected amount of trapped water depends on a structural model of fibrils that is considered (i), on the assumption that all (even small and hydrophobic) cavities are filled with water (ii), and on whether the trapped water is strictly sequestered from the bulk solvent or is in a dynamic equilibrium with the surrounding environment (iii). One source of discrepancy is the fact that FT-IR spectroscopy is a global probe yielding an averaged picture of the conformational and hydrational state of protein, as opposed to cryoelectron microscopy providing detailed information about an arbitrarily chosen specimen (e.g., ref *42*). For instance, in the context of the fibrillation structural polymorphism inherent to insulin (*44*), the fibril consisting of four protofilaments wounding around the large central (and possibly filled with water) canal (*42*) may be statistically underrepresented in actual amyloid sample. A structural destabilization or imperfect alignment of protofilaments would be followed by fast elution of the trapped water with bulk solvent. While the possibility that a similar event is responsible for the vanishing of the D−O−D band intensity in Figure 5 cannot be ruled out, the existence of slowly exchanging or "leaking" water molecules would likely be accompanied by the presence of slowly exchanging amide protons, which as aforementioned is not the case of insulin amyloid. Filling a very tiny and nonpolar (no hydrogen bonding to the walls) cavity with water would face enormous thermodynamic barriers related to formation of the highly frustrated liquid. In terms of hydrodynamics, this would give rise to strong capillary forces pushing water out of cavities. The thermodynamic cost of formation of a structure dotted with empty cavities (void volumes) depends on hydrostatic pressure and may be negligible under ambient conditions. Under sufficiently high hydrostatic pressure, this would become a prevailing thermodynamic contribution disfavoring protein aggregation, which is in accordance with the studies showing that high hydrostatic pressure prevents insulin fibrillation (*18*). In fact, high-pressure dissociation of α-synuclein and transthyretin fibrils has been related directly to the presence of water-excluded cavities by Foguel et al. (*32*). Although FT-IR can detect water molecules as such, its limit of detection is rather high. We estimate that our approach would be useless (even with a longer spectral path length) for detection of water at a concentration 2 orders of magnitude below the values claimed by Perutz et al. (*41*). On the other hand, a highly dispersed water, e.g., in a form of thin monomolecular "chains" running through the fibrils' interior that would escape the detection limit of this method, is extremely unlikely from the thermodynamic point of view. Unsaturated hydrogen bonding and topological restriction within amyloid would result in positive enthalpy and negative entropy changes in molecules transferred against capillary forces from the bulk water into tight cavities.

In conclusion, through the application of FT-IR spectroscopy and H−D exchange in studying insulin fibrillation, we were able to gain new insights into order−disorder boundaries in the aggregation-prone state. The FT-IR-monitored H−D exchange accompanying seeded fibrillation under ambient conditions revealed a dramatic acceleration of the isotopic exchange at the intermediate conformational stage. This proves that structural disorder must occur prior to fibrillation, even if protein molecules are not destabilized en masse, e.g., by high temperatures. This experimental approach may be particularly valuable in addressing some debated structural concepts in the field of amyloid research, such as the three-dimensional domain swapping (*45*), wherein the amount of structural disruption taking place upon elongation of amyloid is confined to the hinge region connecting two domains of an amyloidogenic protein. We have also shown that FT-IR spectra of bending modes of heavy water furnish a convenient and universal probe of water in amyloid cavities. In this work, no water was detected in insulin fibrils, but the same methodology can be applied to the many other protein systems and as such can provide useful and unique complementary information in infrared studies on protein amyloidogenesis.

ACKNOWLEDGMENT

We are grateful to Mrs. Agnieszka Galinska-Rakoczy for her help with TEM.

SUPPORTING INFORMATION AVAILABLE

Mid-infrared spectra of light (H_2O) and heavy (D_2O) water. This material is available free of charge via the Internet at http://pubs.acs.org.

REFERENCES

1. Uversky, V. N., and Fink, A. L. (2004) Conformational constraints for amyloid fibrillation: The importance of being unfolded, *Biochim. Biophys. Acta 1698*, 131−153.
2. Goers, J., Permyakov, S. E., Permyakov, E. A., Uversky, V. N., and Fink, A. L. (2002) Conformational prerequisites for α-lactalbumin fibrillation, *Biochemistry 41*, 12546−12551.
3. Fandrich, M., Fletcher, M. A., and Dobson, C. M. (2001) Amyloid fibrils from muscle myoglobin: Even an ordinary globular protein can assume a rogue guise if conditions are right, *Nature 410*, 165−166.
4. Fandrich, M., and Dobson, C. M. (2002) The behaviour of polyamino acids reveals an inverse side chain effect in amyloid structure formation, *EMBO J. 21*, 5682−5690.

5. Ritter, C., Maddelein, M. L., Siemer, A. B., Luhrs, T., Ernst, M., Meier, B. H., Saupe, S. J., and Riek, R. (2005) Correlation of structural elements and infectivity of the HET-s prion, *Nature 435*, 844−848.
6. Nazabal, A., Maddelein, M. L., Bonneu, M., Saupe, S. J., and Schmitter, J. M. (2005) Probing the structure of the infectious amyloid form of the prion-forming domain of HET-s using high-resolution hydrogen/deuterium exchange monitored by mass spectrometry, *J. Biol. Chem. 280*, 13220−13228.
7. Carulla, N., Caddy, G. L., Hall, D. R., Zurdo, J., Gairi, M., Feliz, M., Giralt, E., Robinson, C. V., and Dobson, C. M. (2005) Molecular recycling within amyloid fibrils, *Nature 436*, 554−558.
8. Li, R. H., and Woodward, C. (1999) The hydrogen exchange core and protein folding, *Protein Sci. 8*, 1571−1590.
9. Krantz, B. A., Moran, L. B., Kentsis, A., and Sosnick, T. R. (2000) D/H amide kinetic isotope effects reveal when hydrogen bonds form during protein folding, *Nat. Struct. Biol. 7*, 62−71.
10. Hoshino, M., Katou, H., Hagihara, Y., Hasegawa, K., Naiki, H., and Goto, Y. (2002) Mapping the core of the β_2-microglobulin amyloid fibril by H/D exchange, *Nat. Struct. Biol. 9*, 332−336.
11. Yamaguchi, K. I., Katou, H., Hoshino, M., Hasegawa, K., Naiki, H., and Goto, Y. (2004) Core and heterogeneity of β_2-microglobulin amyloid fibrils as revealed by H/D exchange, *J. Mol. Biol. 338*, 559−571.
12. Whittemore, N. A., Mishra, R., Kheterpal, I., Williams, A. D., Wetzel, R., and Serpersu, E. H. (2005) Hydrogen−deuterium (H/D) exchange mapping of A-β(1−40) amyloid fibril secondary structure using nuclear magnetic resonance spectroscopy, *Biochemistry 44*, 4434−4441.
13. Del Mar, C., Greenbaum, E. A., Mayne, L., Englander, S. W., and Woods, V. L. (2005) Structure and properties of α-synuclein and other amyloids determined at the amino acid level, *Proc. Natl. Acad. Sci. U.S.A. 102*, 15477−15482.
14. Kheterpal, I., Lashuel, H. A., Hartley, D. M., Wlaz, T., Lansbury, P. T., and Wetzel, R. (2003) Aβ protofibrils possess a stable core structure resistant to hydrogen exchange, *Biochemistry 42*, 14092−14098.
15. Tito, P., Nettleton, E. J., and Robinson, C. V. (2000) Dissecting the hydrogen exchange properties of insulin under amyloid fibril forming conditions: A site-specific investigation by mass spectrometry, *J. Mol. Biol. 303*, 267−278.
16. Zandomeneghi, G., Krebs, M. R. H., Mccammon, M. G., and Fandrich, M. (2004) FTIR reveals structural differences between native β-sheet proteins and amyloid fibrils, *Protein Sci. 13*, 3314−3321.
17. Dzwolak, W., Smirnovas, V., Jansen, R., and Winter, R. (2004) Insulin forms amyloid in a strain-dependent manner: An FT-IR spectroscopic study, *Protein Sci. 13*, 1927−1932.
18. Dzwolak, W., Ravindra, R., Lendermann, J., and Winter, R. (2003) Aggregation of bovine insulin probed by DSC/PPC calorimetry and FTIR spectroscopy, *Biochemistry 42*, 11347−11355.
19. Kardos, J., Okuno, D., Kawai, T., Hagihara, Y., Yumoto, N., Kitagawa, T., Zavodszky, P., Naiki, H., and Goto, Y. (2005) Structural studies reveal that the diverse morphology of β_2-microglobulin aggregates is a reflection of different molecular architectures, *Biochim. Biophys. Acta 1753*, 108−120.
20. Storkel, S., Schneider, H. M., Muntefering, H., and Kashiwagi, S. (1983) Iatrogenic, insulin-dependent, local amyloidosis, *Lab. Invest. 48*, 108−111.
21. Whittingham, J. L., Scott, D. J., Chance, K., Wilson, A., Finch, J., Brange, J., and Dodson, G. G. (2002) Insulin at pH 2: Structural analysis of the conditions promoting insulin fibre formation, *J. Mol. Biol. 318*, 479−490.
22. Brems, D. N., Brown, P. L., Heckenlaible, L. A., and Frank, B. H. (1990) Equilibrium denaturation of insulin and proinsulin, *Biochemistry 29*, 9289−9293.
23. Millican, R. L., and Brems, D. N. (1994) Equilibrium intermediates in the denaturation of human insulin and two monomeric insulin analogs, *Biochemistry 33*, 1116−1124.
24. Nielsen, L., Khurana, R., Coats, A., Frokjaer, S., Brange, J., Vyas, S., Uversky, V. N., and Fink, A. L. (2001) Effect of environmental factors on the kinetics of insulin fibril formation: Elucidation of the molecular mechanism, *Biochemistry 40*, 6036−6046.
25. Ahmad, A., Millett, I. S., Doniach, S., Uversky, V. N., and Fink, A. L. (2003) Partially folded intermediates in insulin fibrillation, *Biochemistry 42*, 11404−11416.
26. Ahmad, A., Millett, I. S., Doniach, S., Uversky, V. N., and Fink, A. L. (2004) Stimulation of insulin fibrillation by urea-induced intermediates, *J. Biol. Chem. 279*, 14999−15013.
27. Sluzky, V., Tamada, J. A., Klibanov, A. M., and Langer, R. (1991) Kinetics of insulin aggregation in aqueous solutions upon agitation in the presence of hydrophobic surfaces, *Proc. Natl. Acad. Sci. U.S.A. 88*, 9377−9381.
28. Jimenez, J. L., Nettleton, E. J., Bouchard, M., Robinson, C. V., Dobson, C. M., and Saibil, H. R. (2002) The protofilament structure of insulin amyloid fibrils, *Proc. Natl. Acad. Sci. U.S.A. 99*, 9196−9201.
29. Dzwolak, W., Grudzielanek, S., Smirnovas, V., Ravindra, R., Nicolini, C., Jansen, R., Loksztejn, A., Porowski, S., and Winter, R. (2005) Ethanol-perturbed amyloidogenic self-assembly of insulin: Looking for origins of amyloid strains, *Biochemistry 44*, 8948−8958.
30. Fandrich, M., Forge, V., Buder, K., Kittler, M., Dobson, C. M., and Diekmann, S. (2003) Myoglobin forms amyloid fibrils by association of unfolded polypeptide segments, *Proc. Natl. Acad. Sci. U.S.A. 100*, 15463−15468.
31. Arora, A., Ha, C., and Park, C. B. (2004) Insulin amyloid fibrillation at above 100 °C: New insights into protein folding under extreme temperatures, *Protein Sci. 13*, 2429−2436.
32. Foguel, D., Suarez, M. C., Ferrao-Gonzales, A. D., Porto, T. C. R., Palmieri, L., Einsiedler, C. M., Andrade, L. R., Lashuel, H. A., Lansbury, P. T., Kelly, J. W., and Silva, J. L. (2003) Dissociation of amyloid fibrils of α-synuclein and transthyretin by pressure reveals their reversible nature and the formation of water-excluded cavities, *Proc. Natl. Acad. Sci. U.S.A. 100*, 9831−9836.
33. Hirota-Nakaoka, N., Hasegawa, K., Naiki, H., and Goto, Y. (2003) Dissolution of β_2-microglobulin amyloid fibrils by dimethylsulfoxide, *J. Biochem. 134*, 159−164.
34. Barth, A. (2000) The infrared absorption of amino acid side chains, *Prog. Biophys. Mol. Biol. 74*, 141−173.
35. Jackson, M., and Mantsch, H. H. (1991) Beware of proteins in DMSO, *Biochim. Biophys. Acta 1078*, 231−235.
36. Max, J. J., and Chapados, C. (2002) Isotope effects in liquid water by infrared spectroscopy, *J. Chem. Phys. 116*, 4626−4642.
37. Zuber, G., Prestrelski, S. J., and Benedek, K. (1992) Application of Fourier transform infrared spectroscopy to studies of aqueous protein solutions, *Anal. Biochem. 207*, 150−156.
38. Jackson, M., Haris, P. I., and Chapman, D. (1989) Conformational transitions in poly(L-lysine): Studies using Fourier transform infrared spectroscopy, *Biochim. Biophys. Acta 998*, 75−79.
39. Dong, J., Wan, Z., Popov, M., Carey, P. R., and Weiss, M. A. (2003) Insulin assembly damps conformational fluctuations: Raman analysis of amide I linewidths in native states and fibrils, *J. Mol. Biol. 330*, 431−442.
40. MacPhee, C. E., and Dobson, C. M. (2000) Chemical dissection and reassembly of amyloid fibrils formed by a peptide fragment of transthyretin, *J. Mol. Biol. 297*, 1203−1215.
41. Perutz, M. F., Finch, J. T., Berriman, J., and Lesk, A. (2002) Amyloid fibers are water-filled nanotubes, *Proc. Natl. Acad. Sci. U.S.A. 99*, 5591−5595.
42. Jimenez, J. L., Guijarro, J. L., Orlova, E., Zurdo, J., Dobson, C. M., Sunde, M., and Saibil, H. R. (1999) Cryo-electron microscopy structure of an SH3 amyloid fibril and model of the molecular packing, *EMBO J. 18*, 815−821.
43. Nelson, R., Sawaya, M. R., Balbirnie, M., Madsen, A. O., Riekel, C., Grothe, R., and Eisenberg, D. (2005) Structure of the cross-β spine of amyloid-like fibrils, *Nature 435*, 773−778.
44. Jansen, R., Dzwolak, W., and Winter, R. (2005) Amyloidogenic self-assembly of insulin aggregates probed by high-resolution atomic force microscopy, *Biophys. J. 88*, 1344−1353.
45. Liu, Y., and Eisenberg, D. (2002) 3D domain swapping: As domains continue to swap, *Protein Sci. 11*, 1285−1299.

BI060341A